International Global Navigation Satellite Systems Association
IGNSS Conference 2016

Colombo Theatres, Kensington Campus, UNSW Australia
6 – 8 December 2016

A PPP-based Multi-sensor Fusion Positioning Solution for Train Localization

Chengming Jin (1)
School of Electronic and Information Engineering/Beijing Jiaotong University/China
+61 0402706234 & chengming.jin@unimelb.edu.au
Allison Kealy (2)
Department of Infrastructure Engineering / The University of Melbourne /Australia
+61 0383446804 & a.kealy@unimelb.edu.au
Jian Wang (3)
School of Electronic and Information Engineering/Beijing Jiaotong University/China
+86 13810877610 & wangj@bjtu.edu.cn
Baigen Cai (4)
School of Electronic and Information Engineering/Beijing Jiaotong University/China
+86 01051687111 & bgcai@bjtu.edu.cn

ABSTRACT

GNSS-based train positioning is one of the most promising solutions for next generation train control systems, e.g. the European Train Control System (ETCS), Chinese Train Control System (CTCS). The key for implementing GNSS-based positioning solution in railways application are the critical RAMS (Reliability, Availability, Maintainability, and Safety) requirements. This paper proposes a real-time Precise Point Positioning (PPP)-based multi-sensor positioning system, which has property of high availability and safety. Depending on different train operation scenarios, the proposed fusion positioning and integrity check solution are intended to improve the RAMS requirements. The integrity will be always monitored, so that critical RAMS requirements are met seamlessly. The feasible system architectures including real time PPP data transmission and GNSS/Odometer/INS fusion positioning are presented in details.

The results of the developed solution indicate that GNSS/Odometer/INS fusion results in better accuracy (0.76 m, 95%) in comparison with stand-alone INS navigation (15.3 m, 95%). In spite of the fact that Kalman Filter convergence process has an adverse impact on detection, identification and adaptation (DIA) quality control, this paper reveals DIA procedure could be used as an integrity monitoring solution of Kalman Filter-based multi-sensor fusion positioning.

KEYWORDS: Real-time PPP, Multi-sensor Fusion Positioning, Integrity Monitoring, Train Localization

1. INTRODUCTION

GNSS-based navigation solution has been broadly utilized in aviation for decades. Unlike other application fields, GNSS-based railway application, especially safety-critical application, requires rigorous performance requirements. Although GNSS-based train positioning is one of the most promising solutions for next generation train control systems, e.g. the European Train Control System (ETCS), Chinese Train Control System (CTCS), Positive Train Control (PTC) (Alessandro N, etc, 2015). The critical RAMS (Reliability, Availability, Maintainability, and Safety) requirements prevent GNSS from train control system application for: (1).GNSS navigation needs a clean sky in the open space; (2). GNSS integrity, which is originally designed for aviation application, is not compatible with railway safety standards; (3). Unaugmented GNSS, e.g. GPS, BDS (BeiDou Navigation Satellite System), does not have satisfactory accuracy.

In order to solve these problems, Jiang L, etc, (2011) presented an Autonomous Integrity Monitoring and Assurance (AIMA) scheme for integrity assurance of the GNSS-based train integrated positioning system. Martin L and Denis S (2013) described a GNSS/velocity senor-based localization algorithm for safety-relevant services. Alessandro N, etc, (2015) proposed a high integrity augmentation system for train control systems basing on single-difference and double-difference approach. This scheme needs more infrastructures since the system consists of EGNOS and a track-side local augmentation network. It turns out that the GNSS-based safety-critical railway application solutions highly rely on the accuracy. However, traditional GNSS augmentation solutions require massive reference stations, which may be unaffordable for railway authority.

Precise Point Positioning (PPP) is a positioning method that employs widely and available GNSS orbit, clock correction and other correction products to perform point positioning using a single receiver via, e.g. the International GNSS Service (IGS) (Thomas G and Craig R, 2013). Unlike RTK (Real Time Kinematic) PPP is operational worldwide and does not require a reference station (Olivier C, 2012). The post-processed PPP can be as accurate as centimetre level in static mode and decimetre level in kinematic mode. Usually PPP suffers from long convergence time because of the ambiguity resolution (AR), sometimes this process is called as PPP-AR. In recent years, with IGS ultra-rapid orbit, clock and FCBs (Fractional Cycle Biases) products, the focus of PPP has shifted to determining an accurate un-differenced solution in real time (Mohamed AA, 2005 and Kongzhe C, 2005). Currently, the IGS RTS (Real Time Service) correction is available on the internet, other correction products, e.g. MADOCA (Multi-GNSS Advanced Demonstration tool for Orbit and Clock Analysis) are also addressing on a real-time positioning with less than 10 cm accuracy. With the evolution of these products, several software products, which implement the PPP solution, have been developed by different institutes and industries. RTKLIB is probably the most popular one among the similar software packages like P3, GIPSY-OASIS, NRCan PPP, GAPS, etc. Since it is an open source program package for standard and precise positioning with GNSS, and it supports a wide range of standard formats and protocols for GNSS. Above all, it supports static and kinematic PPP for both real-time and post-processing.

In this paper, we propose a PPP-based multi-sensor positioning system, which has property of high availability and safety. Depending on different train operation scenarios, PPP/INS/ODO, PPP/INS or INS/ODO integrated Kalman filter solution is deployed actively. When PPP is available, integrity check solution includes PPP integrity monitoring and innovation-based

Kalman filter fault detection. The proposed fusion positioning and integrity check solution are intended to improve the RAMS requirements.

Finally, the results of the developed solution indicate that when PPP is available, a high accurate train positioning can be provided, when PPP is not available, the INS/ODO integrated scheme can provide accurate position as well as velocity information within a certain interval of time. Whenever train localization is available, its safety is always monitored by the proposed integrity check solution.

2. PPP/INS/ODO Integration Scheme and Algorithm

2.1 General

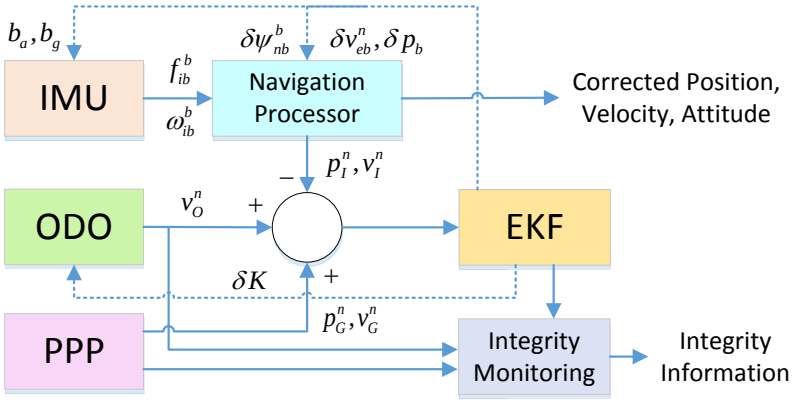

Figure 1. PPP/INS/ODO Integrated Navigation

Although many trials have been made to approach a real-time PPP solution, it still takes much time to converge to an ideal accuracy. On the other hand, before integer ambiguity gets fixed, PPP may have the meter-level accuracy. In addition, in railway application it's not rare that the tunnel, urban canyon blocks the GNSS signals, such that PPP becomes completely unavailable. It's quite often that GNSS is integrated with INS, since the benefits and drawbacks of INS and GNSS are complementary, by integrating them, the advantages of both technologies are combined to give a continuous, high-bandwidth, complete navigation solution with high long- and short-term accuracy (Paul D. Groves, 2013). Another sensor that is broadly mounted on the train is odometer, and in general, train positioning system integrates odometer with other sensors, e.g. balise, radar, to generate position and velocity information with the assistance of track map. Therefore, this paper adopts a PPP/INS/ODO integrated solution.

The PPP/INS/ODO integrated solution is shown in Fig. 1, three scenarios are divided basing on the availability of PPP. In **scenario 1**, GNSS signal is available, but PPP hasn't converged to the nominal accuracy, so the 16 states (3 attitude errors, 3 velocity errors, 3 position errors, 3 accelerometer biases, 3 gyro biases, odometer scalar factor) PPP/INS/ODO extended Kalman filter (EKF) is used. In **scenario 2**, since PPP achieves the ideal accuracy, the 15 states PPP/INS EKF is adopted, thus odometer can be regarded as a redundant check device. While PPP is completely unavailability, which is denoted as **scenario 3**, the 13 states (excluding 3 position errors) INS/ODO EKF is adopted to improve positioning results during the next certain interval of time. Whenever EKF is running, an innovation-based integrity monitoring is always proceeding.

2.2 System State Propagation

The inertial navigation equations will be resolved in the local navigation frame and the position error is expressed in terms of the latitude, longitude, and height, the state vector becomes

$$X_{INS}^{n} = \begin{pmatrix} \delta\psi_{nb}^{b} \\ \delta v_{eb}^{n} \\ \delta p_{b} \\ b_{a} \\ b_{g} \end{pmatrix}, \delta p_{b} = \begin{pmatrix} \delta L_{b} \\ \delta \lambda_{b} \\ \delta h_{b} \end{pmatrix} \tag{1}$$

where the superscript n denotes the local-navigation-frame implementation, the subscript nb denotes from local-navigation-frame to body frame, $\delta\psi_{nb}^{b}$ denotes attitude errors, δv_{eb}^{n} denotes velocity errors, δp_{b} denotes latitude, longitude, height errors, b_{a} denotes accelerometer error and gyro error is denoted by b_{g}. There are lots of inertial navigation books (Paul D. Groves, 2013 and J. A. Farrel, 2008) that deduce the linear relationship between INS error state derivative and error states. Here, the INS system matrix is proved without explanation, a more detailed description can be found in (Paul D. Groves, 2013).

$$F_{INS}^{n} = \begin{pmatrix} F_{11}^{n} & F_{12}^{n} & F_{13}^{n} & 0_{3} & \hat{C}_{b}^{n} \\ F_{21}^{n} & F_{22}^{n} & F_{23}^{n} & \hat{C}_{b}^{n} & 0_{3} \\ 0_{3} & F_{32}^{n} & F_{33}^{n} & 0_{3} & 0_{3} \\ 0_{3} & 0_{3} & 0_{3} & 0_{3} & 0_{3} \\ 0_{3} & 0_{3} & 0_{3} & 0_{3} & 0_{3} \end{pmatrix}_{15\times15} \tag{2}$$

And the INS error states system dynamic model can be described as

$$\dot{X}_{INS}^{n} = F_{INS}^{n} \times X_{INS}^{n} + G_{INS} \times w_{INS} \tag{3}$$

$$G_{INS} = \begin{pmatrix} \hat{C}_{b}^{n} & 0_{3} & 0_{3} & 0_{3} & 0_{3} \\ 0_{3} & \hat{C}_{b}^{n} & 0_{3} & 0_{3} & 0_{3} \\ 0_{3} & 0_{3} & 0_{3} & 0_{3} & 0_{3} \\ 0_{3} & 0_{3} & 0_{3} & \hat{C}_{b}^{n} & 0_{3} \\ 0_{3} & 0_{3} & 0_{3} & 0_{3} & \hat{C}_{b}^{n} \end{pmatrix}_{15\times15} \tag{4}$$

$$w_{INS} = \begin{pmatrix} w_{rg} \\ w_{ra} \\ 0_{3\times1} \\ w_{bad} \\ w_{bgd} \end{pmatrix}_{15\times1} \tag{5}$$

where w_{rg}, w_{ra}, w_{bad} and w_{bgd} are the Gaussian white noise of, respectively, the gyro random noise, accelerometer random noise, accelerometer bias variation and gyro bias variation. $\hat{C}_b^n$ denotes coordinate transformation matrix from body frame to local navigation frame.

The odometer uses an encoder sensor installed at the wheel of the train. The encoder generates pulse signals depending on the rotation of the wheel, the velocity can be measured based on the number of rotations (Jungi Park, 2015). The measured velocity of train (m/s) is calculated by

$$v_{odo,m} = \frac{N \times Sf}{\Delta t} = \frac{N \times (Sf_{ture} + \delta Sf)}{\Delta t} = \frac{N \times Sf_{ture}}{\Delta t} + \frac{\delta Sf}{Sf_{ture}} \times \frac{N \times Sf_{ture}}{\Delta t} = v_{odo,r} + \delta K \times v_{odo,r} \tag{6}$$

where N is the number of pluses, Sf is the nominal conversion factor for encoder, Sf_{true} denotes the real conversion factor, δSf denotes conversion factor error, Δt denotes interval of measurement time. $v_{odo,r}$ denotes real velocity and δK denotes odometer scale factor error. Conversion factor error is the major error sources if the sideslip, ect, of the wheel can be ignored. Error state δK can be regarded as a constant and may be modelled as white noise or Gaussian Markov process (Libin Zhu, Wei Wang, 2010). Here, the white noise model is used

$$\dot{X}_{odo}^n = \dot{\delta K} = 0 \times \delta K + w_{odo} \tag{7}$$

where $w_{odo} = 0$ is assumed here.

Therefore, the continuous time system model in scenario 1 and 2 is described as follows

$$\begin{bmatrix} \dot{X}_{INS}^n \\ \dot{X}_{odo}^n \end{bmatrix} = \begin{bmatrix} F_{INS}^n & 0_{15\times1} \\ 0_{1\times15} & 0 \end{bmatrix} \times \begin{bmatrix} X_{INS}^n \\ X_{odo}^n \end{bmatrix} + \begin{bmatrix} G_{INS} & 0_{15\times1} \\ 0_{1\times15} & 0 \end{bmatrix} \times \begin{bmatrix} w_{INS} \\ w_{odo} \end{bmatrix} \tag{8}$$

And in scenario 3, since only velocity measurement is provided by odometer, the train position states can be eliminated from the estimated states.

2.3 Closed-loop Corrections

In the closed-loop configuration, the estimated error states will be used to correct the inertial navigation solution, IMU outputs and odometer at each iteration.

The corrected inertial navigation solution $\hat{C}_b^n, \hat{v}_{eb}^n$, and $\hat{p}_b$, which comprise the integrated navigation solution, can be obtained from the raw INS solution, $\tilde{C}_b^n, \tilde{v}_{eb}^n$, and $\tilde{p}_b$, using

$$\hat{C}_b^n \approx (I_3 - [\delta\hat{\psi}_{nb}^n \wedge])\tilde{C}_b^n \tag{9}$$

$$\hat{v}_{eb}^n = \tilde{v}_{eb}^n - \delta\hat{v}_{eb}^n \tag{10}$$

$$\hat{p}_b = \tilde{p}_b - \delta\hat{p}_b \tag{11}$$

The IMU-output specific force and angular rate vectors $\tilde{f}_{ib}^b, \tilde{\omega}_{ib}^b$ are corrected by estimated accelerometer and gyro errors b_a , b_g using

$$\hat{f}_{ib}^b = \tilde{f}_{ib}^b - b_a \tag{12}$$

$$\hat{\omega}_{ib}^b = \tilde{\omega}_{ib}^b - b_g \tag{13}$$

The odometer measured velocity $\tilde{v}_{odo,m}^b$ can be corrected by estimated scale factor $\hat{\delta K}$ using

$$\hat{v}_{odo,m}^n \approx \hat{C}_b^n(1-\hat{\delta K}) \times \tilde{v}_{odo,m}^b \tag{14}$$

2.4 Measurement Models

Measurement model describes how the measurements vary with the states. In scenario 1, position measurement, denoted as $p_{P,m}^n$, is provided by PPP while corrected velocity measurement $\hat{v}_{odo,m}^n$ is provided by odometer, so the measurement model is

$$\begin{bmatrix} p_{P,m}^n - \hat{p}_b \\ \hat{v}_{odo,m}^n - \hat{v}_{eb}^n \end{bmatrix} = \begin{bmatrix} 0_{3\times3} & 0_{3\times3} & -I_{3\times3} & 0_{3\times6} & 0_{3\times1} \\ [\hat{v}_{odo,m}^n \wedge] & -I_{3\times3} & 0_{3\times3} & 0_{3\times6} & \hat{v}_{odo,m}^n \end{bmatrix} \times \begin{bmatrix} X_{INS}^n \\ X_{odo}^n \end{bmatrix} + \begin{bmatrix} w_{m,P} \\ w_{m,odo} \end{bmatrix} \tag{15}$$

where $w_{m,P}, w_{m,odo}$ are PPP position and odometer velocity measurement noises respectively. In scenario 2, position and velocity measurements, denoted as $p_{P,m}^n$, $v_{P,m}^n$ respectively, are provided by PPP, so the measurement model is

$$\begin{bmatrix} p_{P,m}^n - \hat{p}_b \\ v_{P,m}^n - \hat{v}_{eb}^n \end{bmatrix} = \begin{bmatrix} 0_{3\times3} & 0_{3\times3} & -I_{3\times3} & 0_{3\times6} \\ 0_{3\times3} & -I_{3\times3} & 0_{3\times3} & 0_{3\times6} \end{bmatrix} \times X_{INS}^n + \begin{bmatrix} w_{m,P} \\ w_{m,odo} \end{bmatrix} \tag{16}$$

In scenario 3, only velocity measurement is provided by odometer, so the measurement model is

$$\hat{v}^n_{odo,m} - \hat{v}^n_{eb} = \begin{bmatrix} [\hat{v}^n_{odo,m} \wedge] & -I_{3\times3} & 0_{3\times6} & \hat{v}^n_{odo,m} \end{bmatrix} \times \begin{bmatrix} X^n_{INS}(7:9,:) = [] \\ X^n_{odo} \end{bmatrix} + w_{m,odo} \tag{17}$$

where $X(a:b,:) = []$ denotes deleting rows of matrix X from a to b.

3. Integrity Monitoring

In comparison with least square (LS)-based receiver autonomous integrity monitoring (RAIM) algorithms, due to the complexity of hybrid GNSS/INS systems, clear integrity requirements and appropriate test procedures have not been developed and defined (MATS BRNNER, 1996). Nevertheless, there are two main approaches (Umar I. Bhatti, 2007), compatible with Kalman filter process, normally employed to determine the test statistic: (1) the use of innovation of the Kalman filter (John Diesel, 1995 and Jan Palmqvist, 1996), and (2) the use of the difference between the main filter solution and the subfilter solution (MATS BRNNER, 1996).

Traditional snapshot RAIM algorithms detect errors or biases in parity space or measurement domain, then the impact of these is calculated by projecting the worst-case offset into the horizontal plane. For Kalman filter systems, it's relatively difficult to project the offset into position error of track-along direction. In addition, a good integrity monitoring approach consists of detection, identification and adaptation (DIA). Therefore, this paper adopts a DIA quality control solution, which can obtain validation of integrated navigation systems. The DIA procedure consisting of three steps is proposed by (Teunissen, 1990). It is a recursive testing procedure that can be used in conjunction with the well-known Kalman filter algorithm, to monitor the integrity in real-time (Christian Tiberius, Peter Joosten).

The detection step of DIA can be compared with the F-test and the identification step can be compared with the w-test, the adaptation step accounts for errors (I. Gillissen, 1996). In this paper, the equation are given without detailed derivation, the complete theoretical background can be obtained in (Teunissen, P.J.G., 1990). And the overall model tests can either be global or local, here only the local test is interpreted since the local test uses current epoch, which makes real-time monitoring possible.

The local test literally detects the observation error, which leaves the validity of the system models to global test. In the detection step, the test statistic t_k at epoch k is shown as follows

$$t_k = \frac{v_k^T Q_{v_k}^{-1} v_k}{m_k} \tag{18}$$

where v_k denotes Kalman measurement innovation, Q_{v_k} denotes covariance matrix of innovation, m_k denotes the number of observations. If the test statistic t_k is larger than the upper σ probability point of the central F-distribution with m_k, ∞ degrees of freedom, an

observation error is detected. For example, in scenario 1, there are six observations, and $\sigma = 0.1\%$ is chosen, then if $t_k \geq 3.74$, an observation error will claim to be detected.

After a detection alarm is raised, the identification tests are processed to identify which one or many observations include errors. The test statistic $t_{k,i}$ at epoch k for $i(th)$ observation reads

$$t_{k,i} = \frac{c_i^T Q_{v_k}^{-1} v_k}{\sqrt{c_i^T Q_{v_k}^{-1} c_i}} \tag{19}$$

where c_i is defined as $(0,...,1,...,0)^T$, the corresponding 1 means that observation is being tested. Once the most likely error has been found, its likelihood needs to be tested by comparing the absolute value of $t_{k,i}$ with the critical value in the double sided normal distribution. For example, the critical value is 3.27 when using a probability of 99.9%. Since more than one error can exist simultaneously, the identification step can be repeated to process (I. Gillissen, 1996).

After identification of the most likely observation error item, adaptation of the recursive navigation filter is needed to eliminate the error or bias $\hat{\nabla}_k$, thus

$$\hat{\nabla}_k = (C_k^T Q_{v_k}^{-1} C_k)^{-1} (C_k^T Q_{v_k}^{-1} v_k) \tag{20}$$

$$x_{k,c}^+ = x_k^+ - K_k C_k \hat{\nabla}_k \tag{21}$$

where C_k is the matrix constructed from vector c_i , if there is one error occurring, $C_k = c_i$. x_k^+ denotes estimated states of Kalman filter and $x_{k,c}^+$ is the corrected states, which will be used as the input for the Kalman filter at next epoch. Covariance matrix of estimated states $P_{X_{k,k}^+}$ is updated as follows (I. Gillissen, 1996)

$$P_{X_{k,k}^+} = P_{X_{k,k}^-} + K_k C_k Q_{\hat{\nabla}_k} K_k{}^T C_k^T \tag{22}$$

$$Q_{\hat{\nabla}_k} = (C_k^T Q_{v_k}^{-1} C_k)^{-1} \tag{23}$$

4. Experiments and Results

4.1 Multi-sensor fusion solutions

An on-site test is done at Princes Park in Melbourne, the trajectory is roughly 800-meter width and the length is around 1.6 km. The results are shown in **Fig** 2 and **Fig** 3. Due to the restriction of paper length, only the simulated test is described in detail.

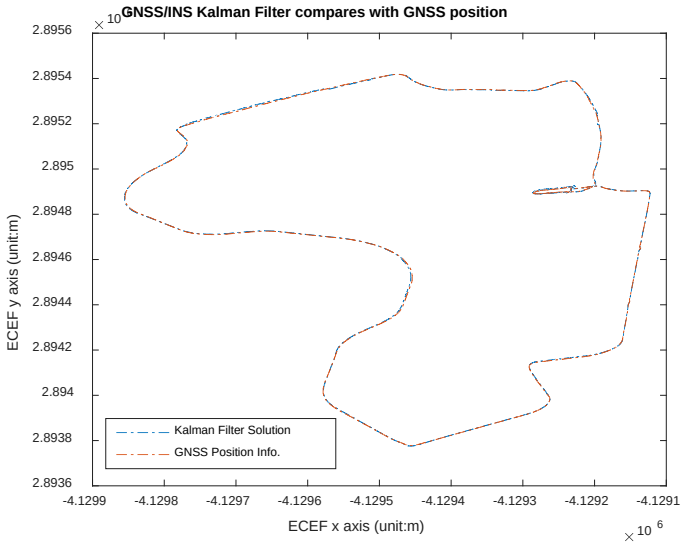

Figure 2 Trajectory of On-site Test

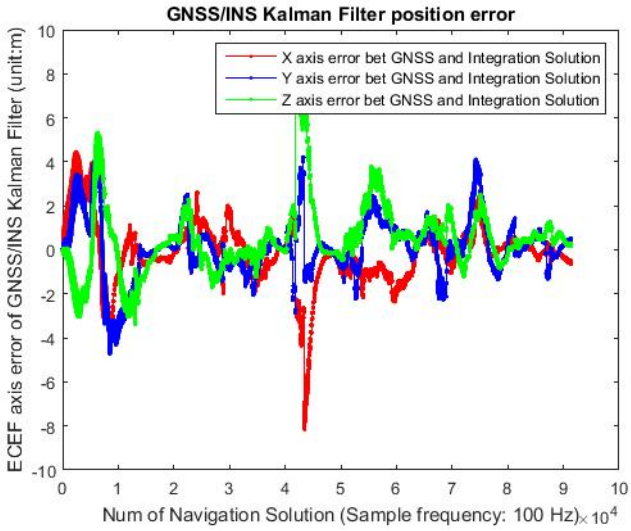

Figure 3 Position Error

The simulated experiments are done basing on the raw data from SPIRENT satellite navigation simulator product (SPIRENT Communications, 2009) as well. Firstly, the stand-alone INS navigation solution is tested. Afterwards, the GNSS/INS navigation solution is tested. Then, GNSS/INS/ODO and INS/ODO navigation solutions are tested respectively. The basic steps are as follows: (1)Using SPIRENT simulator at Beijing Jiaotong University GPS Lab to design a movement trajectory of vehicle; (2)Using corresponding SimGEN software to produce simulated IMU data, which are error-free; (3)PPP and Odo data are produced by adding corresponding error into true position, velocity information; (4)Running experiments. Without specific explanation, the simulated experiments will adapt same parameter settings.

Figure 4 SPIRENT Simulator

In this paper, an eight form trajectory is simulated. As it's shown in **Fig.**5 and **Fig.**6, the deviation shows the effect of gyroscope and accelerometer measured bias and noise. Without any aid, the INS navigation error (15.3 m, 95%) will accumulate and diverge eventually.

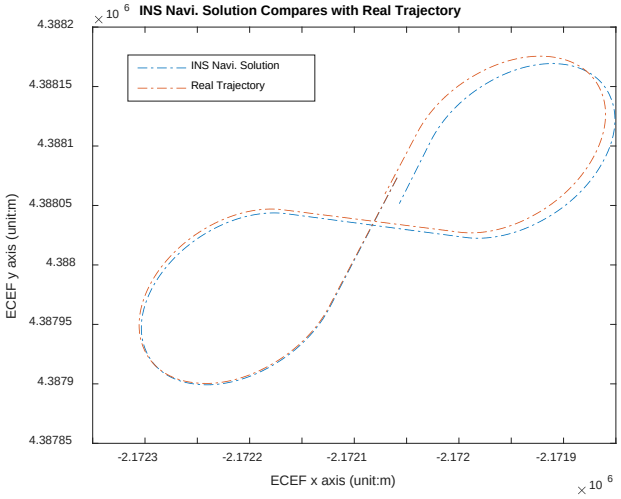

Figure 5 INS Navigation Trajectory

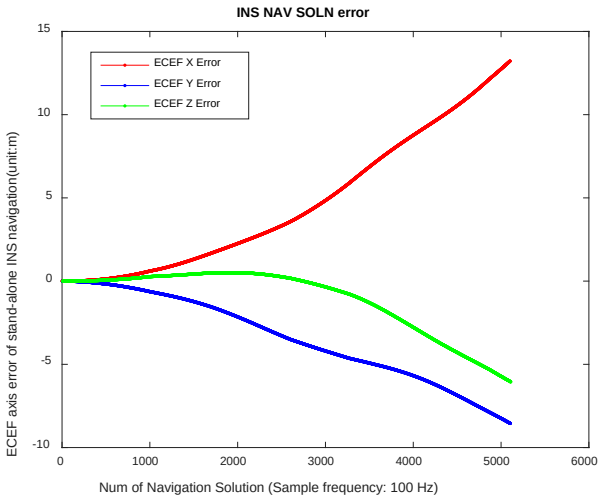

Figure 6 INS Navigation Error

When setting GNSS position standard deviation (SD) as 1 m/s, velocity SD as 0.1 m/s, Kalman filter measurement update frequency as 1 Hz, IMU output frequency as 100 Hz, the GNSS/INS Kalman filter errors (0.7 m, 95%, see **Fig.**7) are stable and much less than that of

stand-alone INS navigation solution. It should be noted that when position are resolved in geodetic latitude, longitude and height, the position error SD needs to be carefully converted into degree instead of meter.

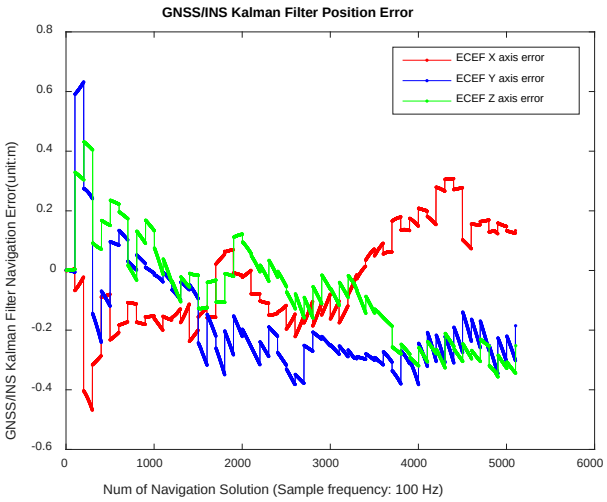

Figure 7 GNSS/INS Kalman Filter Navigation Error

When velocity measurements are provided by odometer with 0.1 m/s SD and 0.1% scale factor bias, **Fig** 8 indicates the GNSS/INS/ODO Kalman filter position error (0.76 m, 95%). Compared with stand-alone INS navigation, GNSS/INS/ODO integration solution improves the accuracy.

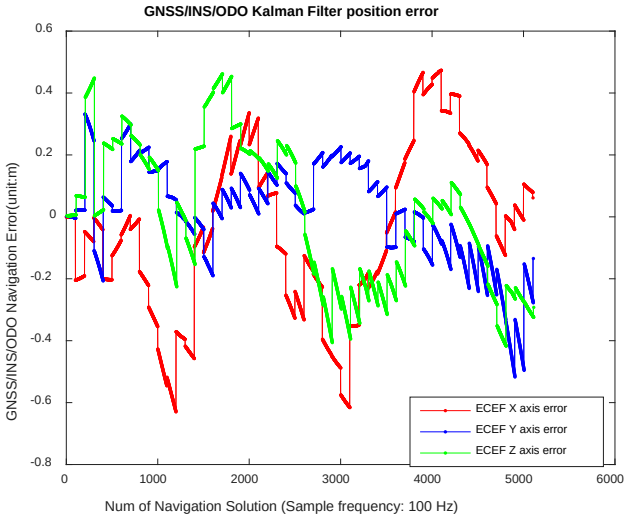

Figure 8 GNSS/INS/ODO Kalman Filter Navigation Error

When the PPP is unavailable, only velocity measurements are provided by odometer, with 100 Hz measurement update, the INS/ODO Kalman filter position error (1.79 m, 95%) is shown in **Fig** 9. In contrast with **Fig** 6, INS/ODO integrated solution improves the INS accumulated error and gives a better positioning solution. Since only inertial sensors are used, the accumulated attitude error will collapse the filter eventually.

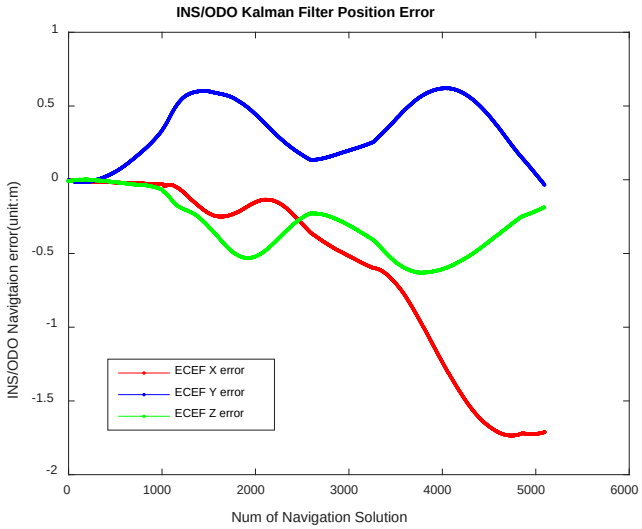

Figure 9 INS/ODO Kalman Filter Navigation Error

4.2 Integrity Monitoring

In this section, the local tests of the GNSS/INS integrated navigation integrity monitoring are done by adding biases with different magnitude into GNSS measurements. When adding corresponding measurement bias into position observation randomly, the results are given in **Table** 1. If the bias is very small, then the success rate of detection is low, when the bias is moderate, the success rate is 98.04%, actually all of the missed detection happen in the first iteration of Kalman filter, which means the convergence process of Kalman filter can affect the detection performance. Thus if a real-time integrity monitoring is required, the convergence problem has to been solved someway like overlapping the integrity check process of contiguous scenarios.

Table 1 Local Test Results with Position Bias

Bias (unit: degree)	Detected	Missed Detection	Success Rate
0	1000	20	98.04%
0.0000001	77	943	7.54%
0.000001	1000	20	98.04%
0.1	1000	20	98.04%
0.5	1000	20	98.04%
10	1020	0	100%

Similar to position bias case, the velocity bias detection is affected by the convergence process of Kalman filter.

Table 2 Local Test Results with Velocity Bias

Bias (unit: m/s)	Detected	Missed Detection	Success Rate
0	1000	20	98.04%
0.1	134	886	13.13%
0.5	1000	20	98.04%
1	1020	0	100%

5. CONCLUSIONS

This paper proposes a PPP-based multi-sensor integrated navigation solution, which is applicable for railway applications. The PPP will improve the accuracy of localization determination. In the meanwhile, Kalman filter-based integrated solution can improve the availability. A DIA quality control is introduced to the Kalman filter iteration process, so that the integrity is always been monitoring. The simulated and on-site tests proof that the methods this paper described is valid and practical.

Since the PPP as well as Kalman filter needs time to converge, thus making the integrity monitoring unstable. More details concerned with this convergence issue need to be studied to further improve the validity of integrity monitoring. Above all, PPP-based navigation solution is promising in railways, since in comparison with differential GNSS or traditional localization method, it can mitigate the dependency on track-sided equipment, although the convergence issue obstructs the achievement of reliable localization solution in safety-critical applications in railways. In addition, the performance of integrated navigation solution shall be further validated in railway scenarios such as multi-path, tunnel.

ACKNOWLEDGEMENTS

This work was supported by National Natural Science Foundation of China (U1334211), International Science & Technology Cooperation Program of China (2014DFA80260), China Railway Corporation science and technology development plan (2015X010-A, 2015X010-B), the China Scholarship Council (Grant No. CSC 201507090010).

REFERENCES

Alessandro N, Salvatore S, Umberto M (2015) GNSS and Odometry Fusion for High Integrity and High Availability Train Control Systems, Proceedings of the 28th International Technical Meeting of The Satellite Division of the Institute of Navigation (ION GNSS+ 2015), Tampa, 639 – 648

Jiang L, Tao T, BaiGen C, Jian W, DeWang C (2011) Integrity assurance of GNSS-based train integrated positioning system, *Science China Technological Sciences* 54(7): 1779-1792

Martin L, Denis S (2013) Algorithms and concepts for an onboard train localization system for safety-relevant services, IEEE International Conference on Intelligent Rail Transportation (ICIRT), Beijing, 65 - 70

Alessandro N, Roberto C, Pietro S (2015) High Integrity Two-tiers Augmentation Systems for Train Control Systems, Proceedings of the ION 2015 Pacific PNT Meeting, Honolulu, 434 – 453

Thomas G, Craig R (2013) Real Time Precise Point Positioning: Are We There Yet ?, IGNSS Symposium, Gold Coast

Olivier C (2012) One-Centimeter Accuracy with PPP, *Inside GNSS*, 49-54

Mohamed AA (2005) Precise point positioning using un-differenced code and carrier phase observations, *Ph.D. Thesis*, School of Engineering, University of Calgary, Alberta.

Kongzhe C and Yang G (2005) Real-Time Precise Point Positioning Using Single Frequency Data, Proceedings of the 18th International Technical Meeting of the Satellite Division of The Institute of Navigation (ION GNSS 2005), Long Beach, 1514 – 1523

Paul D. Groves (2013) *Principles of GNSS, Inertial, and Multisensor Integrated Navigation Systems* (Second Edition), ARTECH HOUSE, London, 800pp

J. A. Farrel (2008) *Aided Navigation: GPS with High Rate Sensors*. The McGraw Hill, 530pp.

Jungi Park, DongSun Lee, Chansik Park (2015) Implementation of Vehicle Navigation System using GNSS, INS, Odometer and Barometer, JPNT 4(3): 141-150

Libin Zhu, Wei Wang (2010) CDGPS-Based Calibration of Odometer's Scale Factor with Temperature for Vehicle Navigation System, *International Conference on Optoelectronics and Image Processing*, Haikou, 317-320

MATS BRNNER (1996) Integrated GPS/Inertial Fault Detection Availability, *Journal of The Institute of Navigation* 43(2):111-130

Umar I. Bhatti, Washington Y. OchiengEmail, Shaojun Feng (2007) Integrity of an integrated GPS/INS system in the presence of slowly growing errors. Part I: A critical review, GPS solution 11: 173-181

John Diesel, Janet King (1995) Integration of Navigation Systems for Fault Detection, Exclusion, and Integrity Determination - Without WAAS, *Proceedings of the 1995 National Technical Meeting of The Institute of Navigation*, Anaheim, 683 – 692

Jan Palmqvist (1996) Integrity Monitoring of Integrated Satellite/Inertial Navigation Systems Using the Likelihood Ratio, *ION GPS 1996*, Kansas, 1687 – 1696

Teunissen, P.J.G. (1990) Quality Control in Integrated Navigation Systems, *IEEE Aerospace and Electronic Systems Magazine* 5(7): 35-41

Christian Tiberius, Peter Joosten. Quality control and integrity, Delft school, Delft University of Technology, Delft.

Teunissen, P.J.G. (1990) Some aspects of Real-Time Model Validation Techniques for Use in Integrated Systems, *Proceedings of the AIG-Symposium on Kinematic Systems in Geodesy, Surveying and Remote Sensing*, Baff, 191-200

I. Gillissen, I. A. Elema (1996) Test Results of DIA: A Real-Time Adaptive Integrity Monitoring Procedure, Used in an Integrated Naviation System, *International Hydrographic Review* LXXIII(1): 75-103

Teunissen, P.J.G. (1990) An Integrity and Quality Control, *Procedure for Use in Multi Sensor Integration. Proceedings of ION GPS-90*, Colorado, 513-522

SPIRENT Communications (2009) SIMGEN Software User Manual, *Report*, SPIRENT Communications, Crawley, United Kingdom.